Self-Assembly

DOI: 10.1002/anie.201000212

Peptides Organized as Bilayer Membranes

*W. Seth Childers, Anil K. Mehta, Rong Ni, Jeannette V. Taylor, and David G. Lynn**

The spontaneous dissipative emergence of supramolecular order underpins all of biology.[1] From the organizing potential of two-dimensional phospholipid membranes to the information-rich DNA helices, from the mechanical actin and tubulin cables to the structural collagen and elastin networks, these self-assembling asymmetric arrays define the architectures of all cells and tissues. Recent covalent hybrids of traditional biological macromolecular families (e.g., nucleic acids with proteins[2] and proteins with lipids[3]) have created novel self-assembling materials, but it has been the models of short peptides as structural[4] and functional[5] bilayer membranes that have created the longest-range order. Yet, little direct proof exists for end-to-end peptide termini interactions in proposed structural models.[6] Herein we present solid-state NMR approaches that directly constrain the KLVFFAL intermolecular paracrystalline arrangement and provide the first unequivocal support for a bilayer architecture.

The nucleating core of the Alzheimer's disease amyloid-β peptide known as Aβ(16–22), KLVFFAE,[6b,c,7] and its E22L congener KLVFFAL assemble as micrometer-long nanotubes (Figure 1a).[4b,6c] Cross-sectioning of epoxy resin embedded KLVFFAL tubes highlights the (4 ± 1) nm wall thickness (Figure 1b) and (45 ± 10) nm diameter, consistent with previous determinations of (4.3 ± 1) nm wall thickness and 38 nm diameter by solution small-angle scattering (SAXS) measurements.[4b,6c] With a maximally extended peptide length of about 2 nm, the end-to-end peptide termini stacking of two amyloid sheets would create a 4 nm thick bilayer,[4b,6c] while additional termini stacking would create thicker tube walls (see Figure S1 in the Supporting Information). Together these results suggested that KLVFFAE peptides may interact through termini interaction to form a peptide bilayer.[4b]

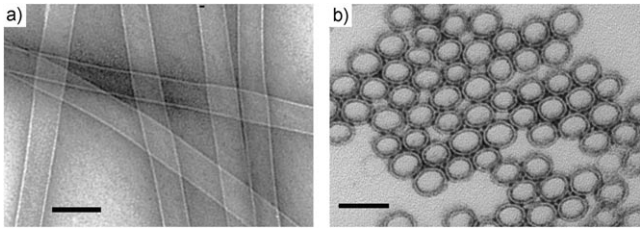

Figure 1. a) Uranyl acetate negatively stained TEM image of dried and flattened KLVFFAL nanotubes (bar = 100 nm) and b) cross-sectioned, epoxy resin embedded assemblies oriented perpendicular to the tube long axis (bar = 100 nm).

A series of solid-state NMR measurements revealed an antiparallel one residue out-of-register β sheet (Figure 2a) and oriented diffraction measurements established a sheet–sheet lamination distance of 9.9 Å (Figure 2b),[6c] but no evidence for a bilayer was apparent in these measurements. Building on these constraints, carbonyl ^{13}C labels were introduced as N-terminal acetates, yielding [1-^{13}C]CH_3CO-K[^{15}N]LVFFAE-NH_2, to directly measure ^{13}C–^{13}C contacts predicted by the bilayer model (Figure 3b). Double Quantum Filtered DRAWS[8] (DQF-DRAWS) analyses of the assembled nanotubes (Figure 3a) supplied homonuclear dipolar couplings (>30 Hz) consistent with ^{13}C–^{13}C distances of <6 Å. As the ^{13}CO acetate neighbors along the H-bonding (9.4 Å) and lamination axes (9.9 Å) are too far to have any observable coupling (Figure 2 and Figure S2 in the Supporting Information), this interaction can be assigned to intermolecular contacts across the bilayer interface (Figure 3). Indeed, when the DQ built-up curves were fit to a spin system (including the effects of measured DQ relaxation;[9] Figure S3 in the Supporting Information) approximating an infinite array of acetates, an interdigitated structure with ^{13}CO–^{13}CO distances of (5.2 ± 0.3) Å was assigned (Figure 3b). Similarly, the congener peptide KLVFFAE also contains a leaflet interface with acetate carbonyl ^{13}C atoms separated by (5.1 ± 0.3) Å (Figure S4 in the Supporting Information).

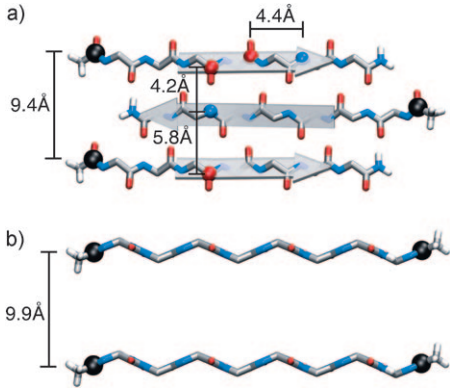

Figure 2. a) β-Sheet structural model with distance constraints[6c] (from diffraction: red spheres, from NMR: blue spheres). Acetate carbonyl labeling scheme (black spheres) to probe the bilayer interface. b) β-Sheet structural model rotated 90° to visualize the lamination of two sheets.

As both KLVFFAE and KLVFFAL contain a leaflet interface, this suggests that a cooperative inter-leaflet K–E interaction is not essential for bilayer formation. To further

[*] W. S. Childers, A. K. Mehta, R. Ni, J. V. Taylor, Prof. D. G. Lynn
Department of Chemistry and Biology, Emory University
1515 Dickey Drive, Atlanta, GA 30332 (USA)
E-mail: david.lynn@emory.edu
Homepage: http://www.chemistry.emory.edu/faculty/lynn.html

Supporting information for this article is available on the WWW under http://dx.doi.org/10.1002/anie.201000212.

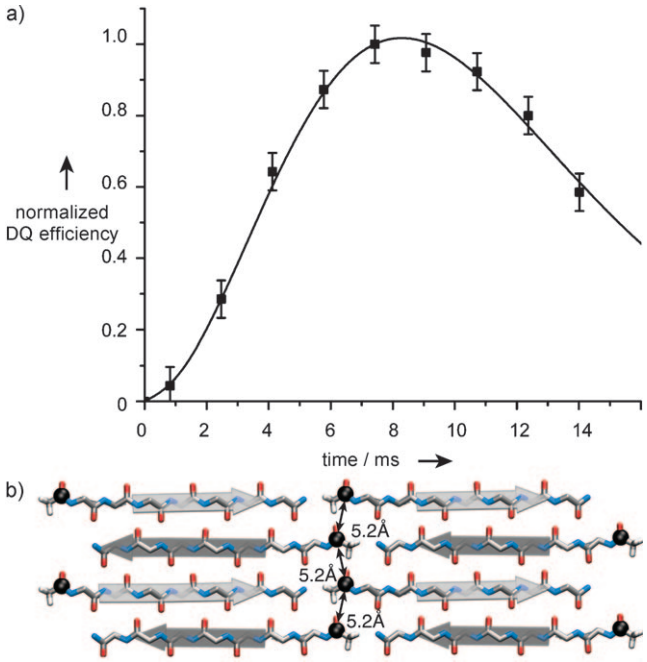

Figure 3. a) ^{13}C DQF-DRAWS of 1.0 mM [1-^{13}C]CH_3CO-K[^{15}N]LVFFAL-NH_2 peptide nanotubes assembled in 40% acetonitrile containing 0.1% TFA and bundled with Na_2SO_4. The solid line is the simulated DQF-DRAWS curve for a ^{13}C–^{13}C distance of 5.2 Å and $T_2DQ = 6.8$ ms. b) Structural model derived from the bilayer DRAWS experiment with the acetate carbonyl groups (black spheres) and distance constraints (arrows and text) highlighted.

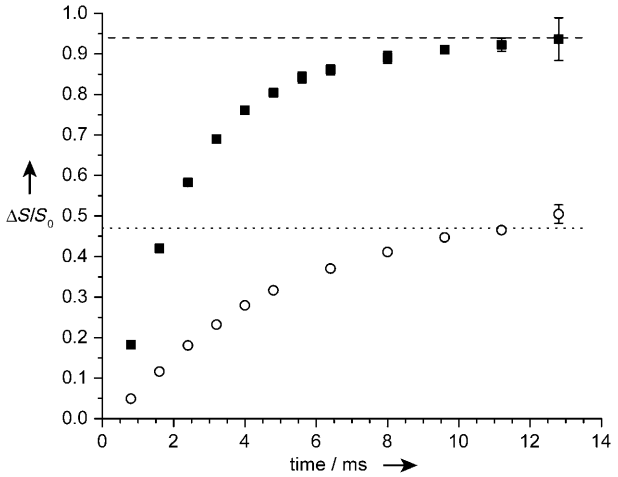

Figure 4. $^{13}C\{^{19}F\}$ REDOR of [1-^{13}C]CH_3CO-KLVFFAL-NH_2 tubes in 40% acetonitrile containing 0.1% TFA. Black squares are for tubes bundled with a single aliquot of Na_2SO_4 and hollow circles are for bundling by slow addition of Na_2HPO_4. The dashed black horizontal line at a $\Delta S/S_0$ value of 0.94 represents dephasing of 100% of the acetate carbonyl ^{13}C nuclei (see Experimental Section). The dotted horizontal line at a $\Delta S/S_0$ value of 0.47 (50% of 0.94) indicates the maximum dephasing if only half of the acetate carbonyl ^{13}C nuclei are close to a CF_3COO^- ion. Unless shown, error bars are the size of the data points.

test this model, we noted that positively charged lysine residues are the least frequently buried residues in protein structures,[10] and must be passivated in the proposed bilayer. Since trifluoroacetic acid (TFA) is used for resin cleavage, HPLC purification, and peptide assembly under acidic conditions (0.1% TFA), its anion could be used to probe the bilayer interface. A single aliquot of 9 mM Na_2SO_4 was used to bundle [1-^{13}C]CH_3CO-K[^{15}N]LVFFAL-NH_2 nanotubes and these assemblies were flash-frozen, and lyophilized[11] for solid-state NMR analysis. $^{13}C\{^{19}F\}$ Rotational-echo double-resonance (REDOR)[12] experiments indicated 100% of the sample contained a 5 to 7 Å distance between the acetate carbonyl carbon atoms and the TFA fluorine atoms (Figure 4, black squares). This result positions the anion of TFA (CF_3COO^-) as lysine's counterion, both within the bilayer interface as well as along the entire aqueous surface of the nanotubes.

We further speculated that the instantaneous increase in Na_2SO_4 from 0 to 9 mM, without pH adjustment, would result in immediate tube bundling, trapping the CF_3COO^- ions at the surface between the tubes. To test this idea, the more weakly bundling salt Na_2HPO_4 was added to the tube solution at a rate of 2 mM h^{-1} up to the final concentration of 9 mM, similar to previous bundling procedures used for SAXS.[11] In this case, REDOR dephasing indicated only about 50% of the *N*-acetyl carbonyl groups retained the same 5 to 7 Å distance to CF_3COO^- (Figure 4, hollow circles), consistent with the other half of the acetate groups being more than 15 Å away from a CF_3COO^- ion (Figure S5 in the Supporting Information). By choosing relatively short REDOR evolution times (14 ms), we were able to accentuate dephasing for only short distances (5–7 Å), minimizing the effects of longer distances (20–25 Å) for the REDOR dephasing spin count[13] (Figure S6 in the Supporting Information) of the number of ^{13}C nuclei close to an ^{19}F nucleus. These analyses indicated that all but a small percentage of the surface CF_3COO^- ions (Figure 5a, green) are being exchanged with phosphate (Figure 5b, orange), while the half that remains buried at the bilayer interface represents a more slowly exchangeable population of CF_3COO^- ions (Figure 5b, green). In contrast for tri- and tetralayer peptide membranes, the $^{13}C\{^{19}F\}$ REDOR curve is predicted to plateau at $\Delta S/S_0$ values of 0.66 and 0.75, respectively (Figure S7 in the Supporting Information). Indeed, gold nanoparticle[14] binding identifies positively charged lysine residues exposed on the membrane surface. As well, Congo red (CR) binding ratios of six peptides for each CR molecule at saturation[15] are consistent with a solvent-exposed surface and a buried CR-inaccessible bilayer interface. This ratio is inconsistent with other leaflet interface models (Figure S8 in the Supporting Information).

These data then establish that peptides can self-assemble into robust bilayer membranes that are morphologically similar to lipids but structurally quite distinct from the traditional lipid assemblies.[16] As the peptides have an antiparallel arrangement,[6c] the inner and outer leaflet faces are patterned as repeating paracrystalline arrays[6c,17] rather than as a homogeneous fluid interface.[18] The patterned faces constituting the bilayer contact surfaces can also be very polar, and in this case, carry high positive charge density passivated with counterions. Such a structure localizes significant functionality within the interior of the bilayer

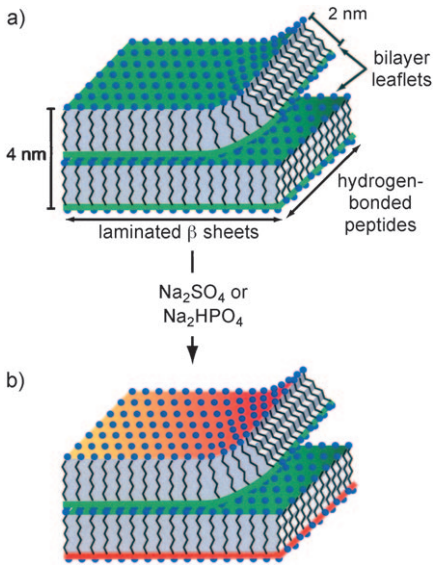

Figure 5. Model of the KLVFFAL peptide bilayer. a) Bilayer structure prior to addition of Na_2SO_4 or Na_2HPO_4. Black lines show the peptide backbone organized as a pleated β sheet, and blue spheres represent the N terminus highlighting the antiparallel β-sheet organization. Green surfaces indicate the presence of CF_3COO^- ions at both surfaces of the bilayer. b) Addition of Na_2SO_4 or Na_2HPO_4 displaces the CF_3COO^- ions (green) on the surface, resulting in a Na_2SO_4 or Na_2HPO_4 rich surface (orange) with CF_3COO^- ions trapped within the bilayer interface.

and opens the possibility for construction of uniquely functional soluble thin-film bilayers.

These patterned surfaces are also created from well-defined β-secondary protein structures.[6c] Unlike lipids[16,19] where the driving force for assembly is weakly directional, the dominant H-bonding axis in KLVFFAE, which is offset from the principle tube axis by 23°,[17,20] provides directionality for association of a relatively large hydrophobic surface area [(406 ± 22) Å^2] of each β strand (Figure S9 in the Supporting Information). In contrast, a surface area of (162 ± 21) Å^2 contributes to the lamination axis of KLVFFAL and this difference probably contributes to the asymmetric organization of the tube. The end-to-end contacts, constituting the bilayer interface, are only (75 ± 11) Å^2 per strand. Monomer organization within each growth plane is influenced by the same forces that control protein folding, including the β-sheet cross-strand pairing rules[21] such as K–E salt bridges,[6c] β-branched residue (Val, Ile) packing[22] and even metal[23] and cofactor binding contributions.[2,11] Taken together, these assemblies further highlight the diverse range of structures that may well underlie the etiology of so many different amyloid diseases,[24] and may now make possible the construction of new patterned bilayer surfaces and functional thin films for many diverse applications.[17]

Experimental Section

Detailed methods for preparing Aβ(16–22)E22L bilayer membranes can be found in the Supporting Information. Peptides were enriched at both the acetate carbonyl carbon and backbone amide nitrogen atoms of L17: [1-^{13}C]CH_3CO-K[^{15}N]LVFFAE and [1-^{13}C]CH_3CO-K[^{15}N]LVFFAL. Only the ^{13}C labels were used to measure distance constraints.

Single-Pulse REDOR: A ^{13}C{^{19}F}-REDOR pulse sequence[25] with EXORCYCLE phase cycling[26] of the single-observe 6 μs ^{13}C (150.8 MHz) π pulse was used to minimize re-introduction of ^{13}C–^{13}C homonuclear dipolar coupling.[27] To compensate for pulse imperfections 5.3 μs ^{19}F REDOR rotor synchronized dephasing π pulses were *xy*8 phase cycled.[28] 83 kHz Spinal64[29] ^{1}H (600.3 MHz) decoupling was applied during REDOR evolution and acquisition. REDOR data points are the integrated sum of center- and sideband peaks. Error bars were calculated using the noise of each spectrum as the maximum peak height deviation. The REDOR $\Delta S/S_0$ plateau reports on the number of observe spins coupled to a dephasing spin. For SO_4^{2-} bundled tubes, the $\Delta S/S_0$ value of less than 1 is consistent with ^{13}C{^{19}F} REDOR experiments on fluoropyruvate (data not shown) and could result from imperfect refocusing of REDOR π pulses and/or interference from multiple CF_3 dephasers and/or a distribution of CF_3–acetate distances, which will be resolved with further experimentation. Details of DQF-DRAWS, peptide synthesis and assembly, and TEM are presented in the Supporting Information.

Received: January 13, 2010
Revised: March 25, 2010
Published online: April 28, 2010

Keywords: nanomaterials · NMR spectroscopy · peptides · self-assembly

[1] a) I. Prigogine, I. Stengers, *Order out of Chaos*, Bantum, New York, **1984**; b) F. Capra, *The Web of Life*, Doubleday, New York, **1996**.
[2] P. Liu, R. Ni, A. K. Mehta, W. S. Childers, A. Lakdawala, S. V. Pingali, P. Thiyagarajan, D. G. Lynn, *J. Am. Chem. Soc.* **2008**, *130*, 16867.
[3] J. D. Hartgerink, E. Beniash, S. I. Stupp, *Proc. Natl. Acad. Sci. USA* **2002**, *99*, 5133.
[4] a) S. Vauthey, S. Santoso, H. Y. Gong, N. Watson, S. G. Zhang, *Proc. Natl. Acad. Sci. USA* **2002**, *99*, 5355; b) K. Lu, J. Jacob, P. Thiyagarajan, V. P. Conticello, D. G. Lynn, *J. Am. Chem. Soc.* **2003**, *125*, 6391; c) S. Santoso, W. Hwang, H. Hartman, S. G. Zhang, *Nano Lett.* **2002**, *2*, 687.
[5] a) X. J. Zhao, Y. Nagai, P. J. Reeves, P. Kiley, H. G. Khorana, S. G. Zhang, *Proc. Natl. Acad. Sci. USA* **2006**, *103*, 17707; b) P. Kiley, X. J. Zhao, M. Vaughn, M. A. Baldo, B. D. Bruce, S. G. Zhang, *PLoS Biol.* **2005**, *3*, 1180; c) K. Matsumoto, M. Vaughn, B. D. Bruce, S. Koutsopoulos, S. G. Zhang, *J. Phys. Chem. B* **2009**, *113*, 75.
[6] a) M. Lopez de La Paz, K. Goldie, J. Zurdo, E. Lacroix, C. M. Dobson, A. Hoenger, L. Serrano, *Proc. Natl. Acad. Sci. USA* **2002**, *99*, 16052; b) J. J. Balbach, Y. Ishii, O. N. Antzutkin, R. D. Leapman, N. W. Rizzo, F. Dyda, J. Reed, R. Tycko, *Biochemistry* **2000**, *39*, 13748; c) A. K. Mehta, K. Lu, W. S. Childers, Y. Liang, S. N. Dublin, J. Dong, J. P. Snyder, S. V. Pingali, P. Thiyagarajan, D. G. Lynn, *J. Am. Chem. Soc.* **2008**, *130*, 9829; d) K. E. Marshall, M. R. Hicks, T. L. Williams, S. V. Hoffmann, A. Rodger, T. R. Dafforn, L. C. Serpell, *Biophys. J.* **2010**, *98*, 330; e) V. Castelletto, I. W. Hamley, R. A. Hule, D. Pochan, *Angew. Chem.* **2009**, *121*, 2353; *Angew. Chem. Int. Ed.* **2009**, *48*, 2317; f) V. Castelletto, I. W. Hamley, P. J. F. Harris, U. Olsson, N. Spencer, *J. Phys. Chem. B* **2009**, *113*, 9978.
[7] T. L. S. Benzinger, D. M. Gregory, T. S. Burkoth, H. Miller-Auer, D. G. Lynn, R. E. Botto, S. C. Meredith, *Proc. Natl. Acad. Sci. USA* **1998**, *95*, 13407.
[8] a) P. V. Bower, N. Oyler, M. A. Mehta, J. R. Long, P. S. Stayton, G. P. Drobny, *J. Am. Chem. Soc.* **1999**, *121*, 8373; b) D. M.

Gregory, M. A. Mehta, J. C. Shiels, G. P. Drobny, *J. Chem. Phys.* **1997**, *107*, 28.
[9] D. M. Gregory, T. L. S. Benzinger, T. S. Burkoth, H. Miller-Auer, D. G. Lynn, S. C. Meredith, R. E. Botto, *Solid State Nucl. Magn. Reson.* **1998**, *13*, 149.
[10] M. Shirota, T. Ishida, K. Kinoshita, *Protein Sci.* **2008**, *17*, 1596.
[11] K. Lu, L. Guo, A. K. Mehta, W. S. Childers, S. N. Dublin, S. Skanthakumar, V. P. Conticello, P. Thiyagarajan, R. P. Apkarian, D. G. Lynn, *Chem. Commun.* **2007**, 2729.
[12] T. Gullion, J. Schaefer, *J. Magn. Reson.* **1989**, *81*, 196.
[13] a) T. M. Forrest, G. E. Wilson, Y. Pan, J. Schaefer, *J. Biol. Chem.* **1991**, *266*, 24485; b) J. R. Garbow, C. A. McWherter, *J. Am. Chem. Soc.* **1993**, *115*, 238.
[14] K. Lu, V. P. Conticello, D. G. Lynn in *Mater. Res. Soc. Synp. Proc. 826E* (Eds.: V. P. Conticello, A. Chilkoti, E. Atkins, D. G. Lynn), Warrensdale, PA, **2004**, p. V1.6.
[15] W. S. Childers, A. K. Mehta, K. Lu, D. G. Lynn, *J. Am. Chem. Soc.* **2009**, *131*, 10165.
[16] T. Hianik, *Acta Phys. Slovaca* **2006**, *56*, 687.
[17] W. S. Childers, R. Ni, A. K. Mehta, D. G. Lynn, *Curr. Opin. Chem. Biol.* **2009**, *13*, 652.
[18] S. J. Singer, G. L. Nicolson, *Science* **1972**, *175*, 720.
[19] J. F. Nagle, S. Tristram-Nagle, *Biochim. Biophys. Acta Rev. Biomembr.* **2000**, *1469*, 159.
[20] J. Dong, K. Lu, A. Lakdawala, A. K. Mehta, D. G. Lynn, *Amyloid* **2006**, *13*, 206.
[21] a) J. S. Merkel, L. Regan, *Folding Des.* **1998**, *3*, 449; b) V. Sieber, G. R. Moe, *Biochemistry* **1996**, *35*, 181.
[22] Y. Liang, S. V. Pingali, A. S. Jogalekar, J. P. Snyder, P. Thiyagarajan, D. G. Lynn, *Biochemistry* **2008**, *47*, 10018.
[23] a) J. Dong, J. E. Shokes, R. A. Scott, D. G. Lynn, *J. Am. Chem. Soc.* **2006**, *128*, 3540; b) J. Dong, J. M. Canfield, A. K. Mehta, J. E. Shokes, B. Tian, W. S. Childers, J. A. Simmons, Z. Mao, R. A. Scott, K. Warncke, D. G. Lynn, *Proc. Natl. Acad. Sci. USA* **2007**, *104*, 13313.
[24] a) L. C. Walker, H. LeVine, M. P. Mattson, M. Jucker, *Trends Neurosci.* **2006**, *29*, 438; b) J. J. W. Wiltzius, M. Landau, R. Nelson, M. R. Sawaya, M. I. Apostol, L. Goldschmidt, A. B. Soriaga, D. Cascio, K. Rajashankar, D. Eisenberg, *Nat. Struct. Mol. Biol.* **2009**, *16*, 973.
[25] Y. Pan, T. Gullion, J. Schaefer, *J. Magn. Reson.* **1990**, *90*, 330.
[26] a) M. Rance, R. A. Byrd, *J. Magn. Reson.* **1983**, *52*, 221; b) N. Sinha, K. Schmidt-Rohr, M. Hong, *J. Magn. Reson.* **2004**, *168*, 358.
[27] a) T. Gullion, S. Vega, *Chem. Phys. Lett.* **1992**, *194*, 423; b) K. L. Wooley, C. A. Klug, K. Tasaki, J. Schaefer, *J. Am. Chem. Soc.* **1997**, *119*, 53.
[28] T. Gullion, D. B. Baker, M. S. Conradi, *J. Magn. Reson.* **1990**, *89*, 479.
[29] B. M. Fung, A. K. Khitrin, K. Ermolaev, *J. Magn. Reson.* **2000**, *142*, 97.

